

Full Length Article

Structural coloration of metallic surfaces with micro/nano-structures induced by elliptical vibration texturing

Yang Yang^a, Yayue Pan^b, Ping Guo^{a,*}^a Department of Mechanical and Automation Engineering, The Chinese University of Hong Kong, Hong Kong, China^b Department of Mechanical and Industrial Engineering, University of Illinois at Chicago, Chicago, IL, USA

ARTICLE INFO

Article history:

Received 8 October 2016

Received in revised form 8 December 2016

Accepted 4 January 2017

Available online 5 January 2017

Keywords:

Structural coloration

Micro-grating

Elliptical vibration texturing

Vibration-assisted machining

ABSTRACT

Creating orderly periodic micro/nano-structures on metallic surfaces, or structural coloration, for control of surface apparent color and optical reflectivity has been an exciting research topic over the years. The direct applications of structural coloration include color marking, display devices, and invisibility cloak. This paper presents an efficient method to colorize metallic surfaces with periodic micro/nano-gratings using elliptical vibration texturing. When the tool vibration is coupled with a constant cutting velocity, controlled periodic ripples can be generated due to the overlapping tool trajectory. These periodic ripples with a wavelength near visible spectrum can act as micro-gratings to introduce iridescent colors. The proposed technique also provides a flexible method for color marking of metallic surfaces with arbitrary patterns and images by precise control of the spacing distance and orientation of induced micro/nano-ripples. Theoretical analysis and experimental results are given to demonstrate structural coloration of metals by a direct mechanical machining technique.

© 2017 Published by Elsevier B.V.

1. Introduction

Surface micro/nano-structures have been widely studied to create functional surfaces for enhanced performance in their tribological, biological, mechanical, and optical properties [1]. Specifically, creating orderly periodic near-subwavelength micro/nano-structures on metallic surfaces, or structural coloration, serves as a physical process for controlling the color and optical reflectivity of metals, which has a variety of potential applications, such as color marking, display devices, and invisibility cloak technology [2–4]. Structural coloration has been attributed to the complex interactions between light waves and surface micro/nano-structures, which has been widely observed in nature, such as the color change of Morpho butterflies and iridescent colors of peacocks' feathers [5]. The structural coloration can be attributed to a range of photonic mechanisms, including plasmonic effects [6,7] and diffraction grating effects. The diffraction-grating induced structural coloration is unique such that it renders an iridescent effect, or the apparent color is dependent on the viewing angle. This paper focuses on the manufacturing and evaluation of structural coloration based on the diffraction grating effect.

Diffraction gratings have been traditionally manufactured by using mechanical ruling [8] and interference lithography [9]. These methods are used to produce extremely uniform and high quality master molds of diffraction gratings for mass production of their replicates. However, these traditional methods are not able to create complex colorful patterns. More recently, researchers have utilized femtosecond lasers for structural coloration by utilizing the laser induced periodic surface structures (LIPSSs). Vorobyev and Guo [10] used a femtosecond laser to render aluminum surfaces to gold, black and grey by structural coloration. By a similar technique, laser-induced periodic surface structures covered with nano-particles were generated on aluminum surfaces resulting in an iridescent effect of aluminum [10]. Ahsan et al. [11] have prepared colorful stainless steel surfaces with periodic micro-holes and micro/nano-ripples induced by femtosecond laser impulses. The orientation of LIPSSs is controlled by changing the laser polarization direction to produce different apparent colors for color marking [2].

The laser induced orderly surface patterns are spontaneously generated during laser irradiation due to the laser-matter interaction. Average spatial intervals of the closely arranged LIPSSs produced by a femtosecond laser locate in the visible spectrum. The interval length of LIPSSs is subjected to the laser wavelength, average fluence, pulse frequency, scanning speed, etc. [12,13]. Structural coloration using LIPSSs can be explained intuitively by

* Corresponding author.

E-mail address: pguo@mae.chk.edu.hk (P. Guo).

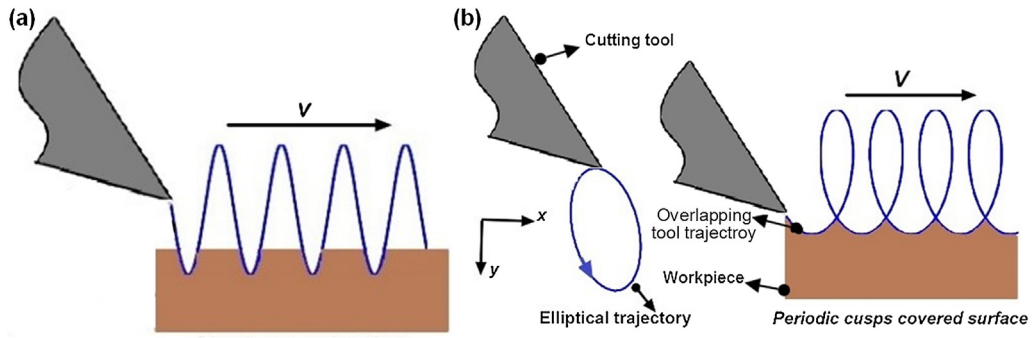


Fig. 1. Process principle: (a) intuitive idea of cutting depth modulation; (b) proposed elliptical vibration texturing using an overlapping tool trajectory.

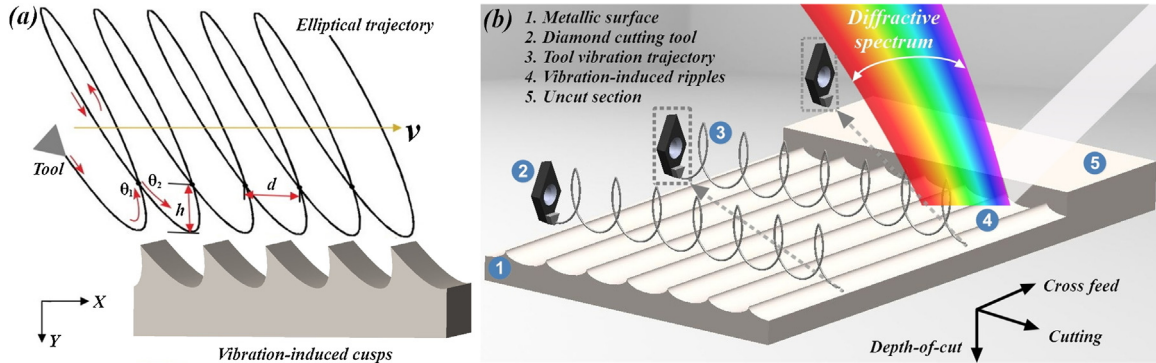


Fig. 2. (a) Geometry definition of vibration-induced cusps and (b) schematic of micro/nano-ripples induced by elliptical vibration texturing process.

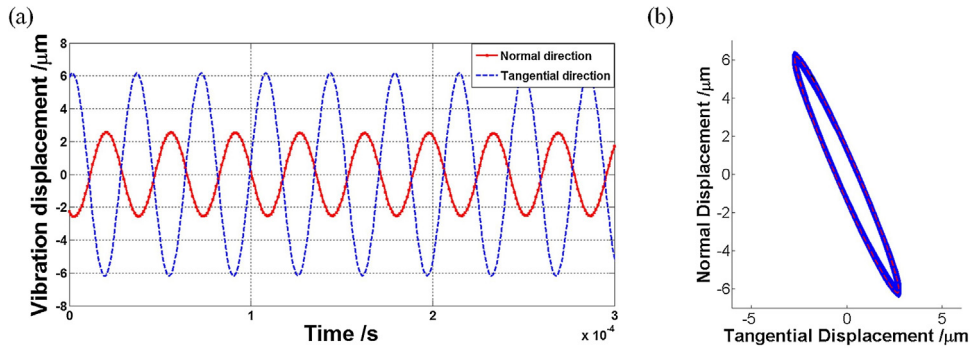


Fig. 3. (a) Response vibration displacements and (b) elliptical trajectory of the cutting tool.

two different factors [13]: (1) the color effect of laser induced nano-particles on top of the micro-gratings, which accounts for the non-iridescent colors; and (2) the grating diffraction effect of LIPSSs, which accounts for the iridescent colors. Iridescent colors due to the periodic structures can be described by the grating equation, which states the relationship between the grating spacing and the angles of diffracted light:

$$d (\sin\theta_i + \sin\theta_m) = m\lambda \quad (1)$$

where d is the grating spacing; m is an integer indicating the diffraction order; θ_i and θ_m are the light incident angle and the angle of diffracted beams of order m , respectively; and λ is the wavelength.

If the incident white light is perpendicular to the surface, the viewing angle of a certain color of wavelength, λ , is given by the diffracted angle maxima, which is given by:

$$\theta_m = \arcsin \left(\frac{m\lambda}{d} \right) \quad (2)$$

The laser induced periodic ripples, though are highly reproducible, suffer from several drawbacks. Firstly, the ripple density or grating spacing, d , which specifies the diffracting resolution, is subjected to the wavelength of laser source. In addition, it is difficult to predict and control the grating spacing and hence limit the technology to produce micro/nano-gratings with arbitrary spacing. Secondly, the produced micro/nano-gratings are semi-regular, which deteriorates the diffraction efficiency, or the color effect. Lastly, the high cost of a femtosecond laser system makes the technology difficult to be adopted by the industry. The above-mentioned problems motivate this paper, which is to develop an efficient manufacturing process with a low-cost setup to produce controllable periodic ripples on metallic surfaces for improving their appearance and optical properties.

In this paper, we demonstrate the fast creation of micro/nano-ripples with wavelength in the UV light, visible and infrared spectrum (300 nm–1300 nm) on metallic surfaces using elliptical vibration texturing, which is a vibration-assisted mechanical cutting process. Original mono-color of metallic surfaces have been

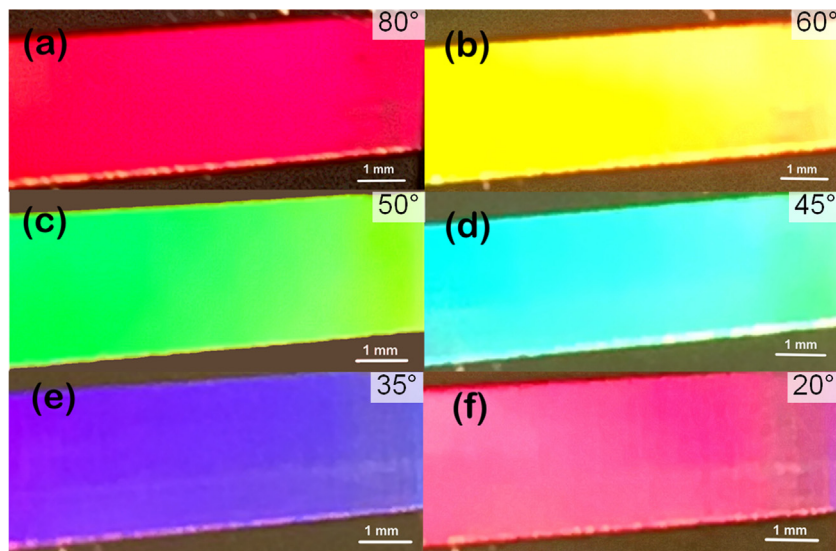


Fig. 4. Images of one textured brass surface with iridescent effect viewing at different angles: (a) red, (b) yellow, (c) green, (d) cyan, (d) purple, and (e) magenta (the white light was shed perpendicular to the workpiece, while the viewing angle is denoted in the figure). (For interpretation of the references to color in this figure legend, the reader is referred to the web version of this article.)

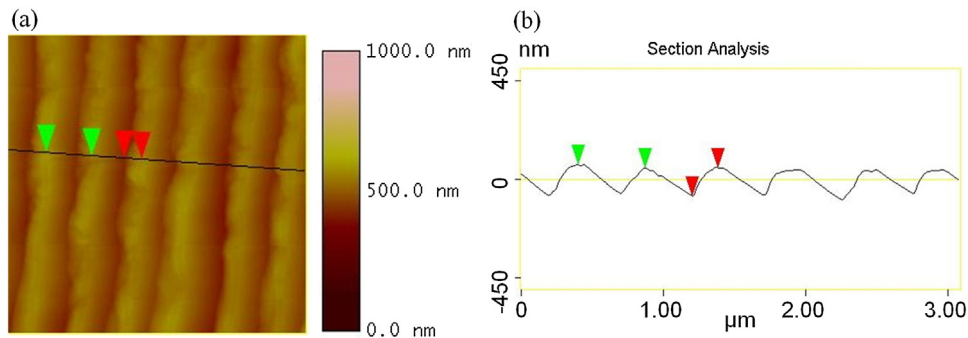


Fig. 5. (a) AFM image of an area of $3 \mu\text{m} \times 3 \mu\text{m}$ of the sample in Fig. 4; and (b) the corresponding cross-section profile of the measured line in (a).

rendered into iridescent appearance using the proposed method. Vibration-induced periodic ripples on metallic surfaces act as micro-gratings for optical reflection and diffraction to achieve an iridescent effect. Compared to the traditional dyeing method, the proposed structural coloration technique makes the processed surface preserve its color longer and insensitive to physical wear or chemical corrosion. Furthermore, it eliminates the usage of any toxic chemical reagents. The proposed technology also provides a flexible method for color marking of metallic surfaces with arbitrary patterns and images. With a suitable combination of different processing parameters, various periodic micro/nano-ripples with different spacing distances and orientations can be concurrently generated on machined surfaces leading to iridescent patterns and pictures. The proposed technique, which could produce fine micro/nano-ripples down to the visible spectrum with fine resolution, could find many applications in micro-optics systems, display devices, functional decoration, information encryption storage, anti-counterfeiting devices, etc.

The principle of the processing technique is first explained. Then the experimental procedures and preliminary results of iridescent samples are demonstrated. The micro-surface morphology and cross-section profiles of machined samples are studied to verify the process principles. Techniques to create colorful patterns and images are discussed and demonstrated, followed by a conclusion of the paper.

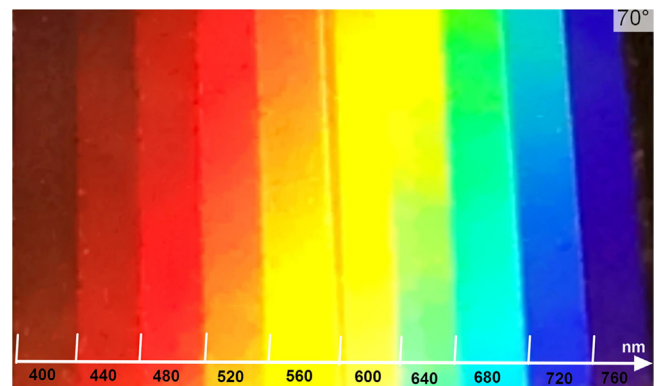


Fig. 6. Color spectrum on brass surface marked by ten segments: each segment has been textured with different spacing distances (from 400 nm to 760 nm).

2. Process principle

The proposed process attempts to use mechanical machining to generate submicron-scale periodic structures for structural coloration. The intuitive idea is to add a modulation to the cutting depth during the shaping operation, as shown in Fig. 1(a), such that periodic structures can be concurrently machined in the direction perpendicular to the cutting direction. The grating spacing can be controlled by either change the modulation frequency or

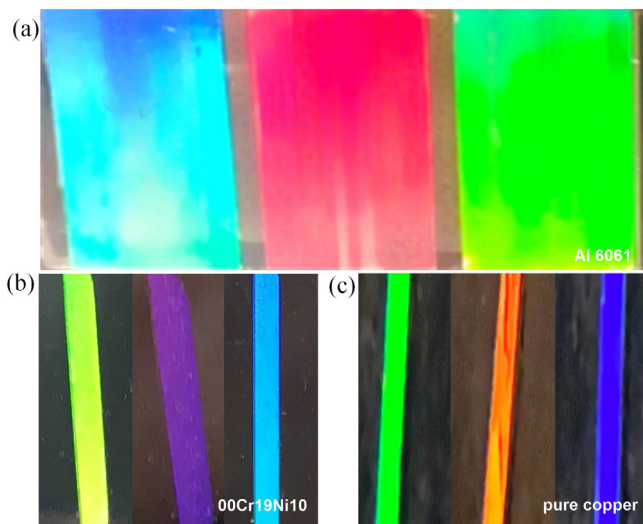


Fig. 7. Iridescent effect achieved on different materials: (a) aluminum alloy, (b) stainless steel, and (c) copper.

the cutting velocity for color marking of complex patterns. This simple concept, however, has not been reported for generation of sub-micron diffraction gratings in the literature mainly due to two reasons. First, there is no proper actuator which could generate fast enough modulation in the depth-of-cut direction. The nominal cutting velocity of the cutting tool is directly proportional to the modulation frequency. It not only determines the process efficiency, but also has a major impact on the machining quality. Commercial fast tool servos, which could generate fast 1D actuation, usually have a bandwidth in the kilohertz range. If we would like to generate diffraction gratings of 500 nm spacing using a 1 kHz motion, the corresponding nominal cutting velocity would be 0.5 mm/s. The efficiency would be unsatisfactory, but more importantly the low cutting velocity may prevent a stable cutting condition and significantly deteriorate the surface quality. Second, mechanical machining conventionally is not favored in processing nano-scale features due to the minimum chip thickness effect [14,15]. When the uncut chip thickness is below a critical value, which is called the minimum chip thickness, no chip will be formed and the material will flow beneath the tool. Even an ultra-fast actuator is available, the uncut chip thickness when machining sub-micron periodic structures will fall below the minimum chip thickness, so that a stable cutting process cannot be established. Due to the above-stated two reasons: (1) technical difficulties in ultra-fast tool actuation and (2) minimum chip thickness effect in micro-cutting mechanics, the principle of cutting depth modulation shown in Fig. 1(a) has not been adopted for generating sub-micron periodic structures.

In this paper, elliptical vibration texturing (EVT) is proposed for fast generation of sub-micron periodic gratings for structural coloration on metallic surfaces. The process principle is shown in Fig. 1(b). When two-dimensional ultrasonic vibration is applied to the cutting tool, periodic cusps will be left on processed surfaces due to the overlapping tool trajectory. This method has been demonstrated for the first time for structural coloration, which could address the aforementioned difficulties. Two-dimensional ultrasonic vibration (28 kHz) was applied to the cutting tool, so that 28 thousand periodic structures could be generated per second; and the nominal cutting velocity would be increased to 14 mm/s for the same 500 nm spacing gratings. More importantly, the two-dimensional vibration would result in the overlapping tool trajectories and the naturally formed periodic cusps left on the process surface. The actual uncut chip thickness thus would be much

greater than the micro-scale feature size as well as the minimum chip thickness. A stable cutting process would be established rather than a ploughing process.

As shown in Fig. 2(a), the machining marks, or periodic cusps, are in the form of orderly ripples, whose orientation is perpendicular to the cutting direction. The ripple spacing can be precisely controlled, which is determined by the ratio of nominal cutting velocity to tool vibration frequency; it is given by:

$$d = (2\pi v) / \omega \quad (3)$$

where v is the nominal tool cutting velocity; and the ω is the tool vibration frequency.

The height of cusps is associated with a process-dependent variable, denoted as the “overlapping ratio” of the tool path. To describe the intersection area of the tool path, one can define the overlapping ratio as the maximal vibration velocity in the cutting direction (X axis) divided by the nominal cutting velocity. Intuitively, the cusp height is inversely related to the overlapping ratio, and positively related to the ripple spacing distance, d . In addition, the overlapping ratio is also associated with the tool vibration amplitude in the tangential direction for a given spacing distance. Typical height values of vibration-induced micro/nano-ripples in the UV to near-infrared spectrum lie in the range of several tens of to several hundreds of nanometers. The coordinates of the cusps can be analytically determined according to Fig. 2(a):

$$A_x \cos\left(\frac{\theta_1 + \theta_2}{2}\right) \sin\left(\frac{\theta_1 - \theta_2}{2}\right) + \frac{v(\theta_1 - \theta_2)}{2\omega} = 0 \quad (4)$$

where A_x is the tool vibration amplitude in cutting direction; θ_1 and θ_2 are two particular angular positions of the tool tip corresponding to the coordinates of the cusps, whose values are between 0 and 2π . Their particular values can be solved numerically. Then the height of the vibration induced cusps is given by:

$$h = A_y (1 - |\sin(\theta_1 + \varphi)|) \quad (5)$$

where A_y is tool vibration amplitude in the cutting depth direction.

By sequential cuttings in parallel lines as shown in Fig. 2(b), the vibration-induced ripples are connected to form incessant long edges due to the overlapping of cutting areas in the cross-feed direction. Periodic micro/nano-ripples with a wavelength from UV to near-infrared spectrum have been concurrently generated on machined surfaces using the proposed EVT process. The geometry and spacing distance of the ripples can be precisely controlled by adjusting the process parameters, so the generated ripples can act as micro/nano-gratings for optical reflection and diffraction to achieve an iridescent effect.

3. Experimental setup and details

The key component in the elliptical vibration texturing process [16,17] is a tertiary motion generator capable of producing elliptical vibration at the tool tip. The device was carefully constructed to possess two orthogonal vibration modes at an identical ultrasonic frequency. Then an elliptical tool trajectory was obtained due to the coupled resonant modes when the device was driven at the coupled resonant frequency. Vibration amplitude up to 10 μm at the ultrasonic frequency in each direction (cutting and depth-of-cut directions) can be achieved. More detailed descriptions of the design and principle of the resonant vibrator can be found in our previous work [18].

Since the induced ripples were at the scale of several hundred nanometers, a commercial single crystal diamond cutting insert was mounted on the tertiary motion generator for the texturing process. The rake and clearance angles of the cutting insert are 0° and 12° , while the nose radius is 509 μm . The high-voltage

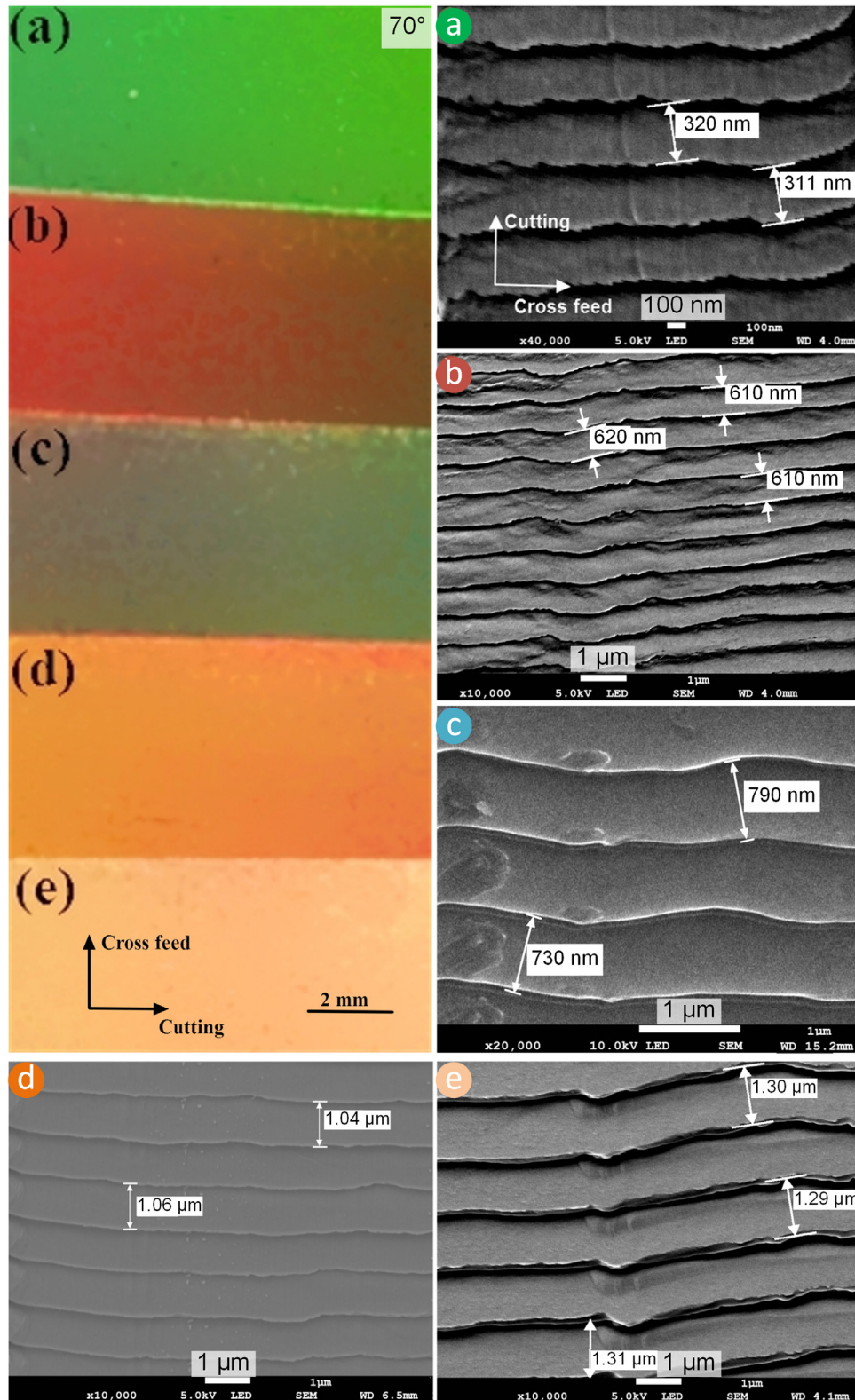


Fig. 8. Five segments with different colors viewed at 70° processed with different cutting velocities; and SEM micrographs of the corresponding surface micro-topography: (a) 300 nm, (b) 600 nm, (c) 750 nm, (d) 1000 nm, and (e) 1300 nm.

excitation signals were generated by a two-channel function generator and then amplified by a piezo amplifier (TREK PZD350A). The amplifier is capable of producing ± 350 V bipolar voltage and ± 200 mA bipolar current. The tertiary motion generator was fixed on an Aerotech linear actuator (ACT115DL), which provides cutting

motion (X axis) during the texturing process. The resolution and repeatability of the linear actuator are 10 nm and $1 \mu\text{m}$, respectively. In order to ensure the optimal vibration performance of the cutting tool, two capacitance displacement sensors from Microsense (Model 5504) were adopted and integrated to the machine setup

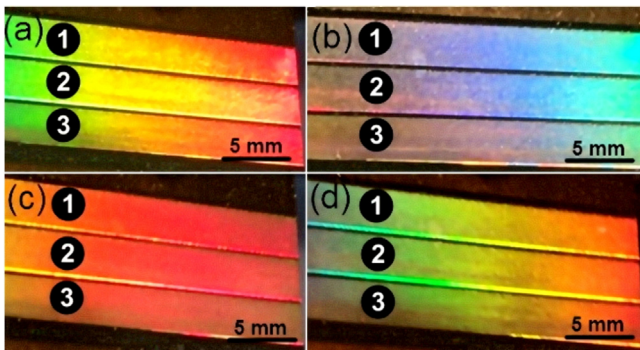


Fig. 9. (a–d) Iridescent effect achieved with the same cutting velocity, cross feed and different nominal depth-of-cuts viewed from different angles. Nominal depth-of-cut: (1) $-3\ \mu\text{m}$; (2) $0\ \mu\text{m}$; and (3) $3\ \mu\text{m}$.

to monitor the dynamic vibration displacement responses of the cutting tool. The measured response signals were transmitted to a NI data acquisition card (NI DAQ PCIe-6361) for further processing through a LabVIEW interface at a sampling rate of 1 MHz.

The workpiece was screwed on an *Aerotech* three-axis motion stage (ANT130-060-L) through a base plate adaptor. Processing parameters of depth-of-cut (Y axis) and cross-feed (Z axis) were set by the three-axis motion stage, which has 1 nm resolution and 75 nm repeatability for each axes. The whole setup was stationed on a vibration isolation table and controlled by an A3200 control system.

A pre-tuning process was necessary for the tertiary motion generator to achieve the ideal vibration performance for the texturing process. Meanwhile, the vibration performance should also be evaluated from time to time during the texturing process to ensure the consistency of tool vibration trajectories. To this end, the tertiary motion generator was carefully calibrated to the designed resonant operation mode. Vibration displacements of the tool tip were recorded using two capacitance displacement sensors in the cutting and depth-of-cut directions. By means of a frequency sweep test, the coupled resonant frequency of the tertiary motion generator was found at 28.0 kHz. The applied sinusoidal voltage amplitudes were set at $\pm 300\ \text{V}$, while the phase difference between the two excitation signals was set at 0° to achieve the largest vibration amplitude in the depth-of-cut direction. The 2D tool trajectories along with the tool displacements in the cutting and depth-of-cut directions are plotted in Fig. 3. The peak-to-peak vibration amplitudes in the depth-of-cut and cutting directions were determined to be $12.0\ \mu\text{m}$ and $4.5\ \mu\text{m}$.

Using the driving parameters obtained from the pre-tuning process, the cutting tool can vibrate along an elliptical trajectory for the following coloration process. It should be noted that specific micro/nano-structures are determined by the excitation signals, process parameters and cutting tool geometry, etc. The particular process parameters, e.g. nominal cutting velocity, cross feed, nominal depth-of-cut, require careful considerations, since the geometry and the vibration frequency of the tool were fixed during the coloration process. As discussed in the principle section, nominal cutting velocity plays a key role in the induced ripple spacing distance and overall grating effect of the colorized metallic samples. Particular cross feeds are selected to link the cusps in the cross-feed direction to form incessant ripples, while the nominal depth-of-cut determines the material removal rate and cutting force. Following the texturing process, all the machined samples were cleaned in an ultrasonic cleaner with acetone at 50°C for 10 min. Color pictures of the textured samples were shot under different observing angles using an iPhone 6s camera under a halogen lamp as the light source. Then the height profile of vibration-induced structures was investi-

gated with a *Multimode* atomic force microscope (AFM) in contact mode, while the surface morphology of textured structures was studied using a *JOEL* scanning electronic microscope (JSM-7800F) with a LED detector and acceleration voltage of 5 kV.

4. Results and discussions

4.1. Process principle verification

Preliminary iridescent effects have been achieved on brass surfaces with a nominal cutting velocity of $14.0\ \text{mm/s}$, cross feed of $50\ \mu\text{m}$ and 0 depth-of-cut, as shown in Fig. 4. An area of $10\ \text{mm} \times 3\ \text{mm}$ has been textured within 3 min due to the ultrasonic vibration frequency of the tool. As seen from the textured results, the brass surface exhibited different vivid colors without any pigment or coating material. Furthermore, the apparent color varied from one viewing angle to another as demonstrated in Fig. 4(a)–(f). In essence, these iridescent effects are attributed to the micro/nano-ripples induced by the elliptical vibration texturing process. Periodic vibration-induced micro/nano-ripples uniformly distributed on the brass surface act as micro-gratings resulting in reflection and diffraction effects. Governed by the diffraction grating equation, the apparent color is determined by the spacing distance, viewing angle, and incident light angle. For a given constant spacing distance and a normal incident angle, the white light with different wavelengths is diffracted along different directions leading to an iridescent effect of metallic surfaces. Light with a longer wavelength appears at a larger diffraction angle, while light with a shorter wavelength appears at a smaller diffraction angle.

In addition, the overall grating effect mainly depends on the grating geometry and grating density. A larger grating density and higher aspect-ratio contribute to a finer grating resolution and a better iridescent effect. Both of the grating density and geometry can be controlled by the proposed technique by adjusting the process parameters. The grating geometry can be partially controlled by the design of tool geometry and fine tuning of the tool vibration trajectory. Fig. 5(a) shows a 3D image of the micro/nano-ripples distributed on the sample in Fig. 4 measured with an AFM, while the corresponding cross-section profile is plotted in Fig. 5(b). The profile resembles the geometry of blazed gratings, and has an average height of $130\ \text{nm}$. On the other hand, the grating density, or grating spacing, can be more easily controlled by adjusting the nominal cutting velocity and is the main parameter to study in this work. The grating density in the presented sample shown in Fig. 4 can be calculated to be 2000 lines/mm, and was measured to be $470\ \text{nm}$ as shown in Fig. 5(b).

In order to find out the range of color which can be reproduced by the proposed technique, a color palette was generated with ten segments whose ripple spacing was from $400\ \text{nm}$ to $760\ \text{nm}$ with an increment of $40\ \text{nm}$. As shown in Fig. 6, when the workpiece was viewed at 70° , the whole visible spectrum can be identified. It should be noted that the spacing distance of generated micro/nano-ripples is not limited to the visible spectrum for achieving an iridescent effect. However, larger spacing distances lead to a lower grating resolution, and a rainbow color effect due to a smaller angular dispersion; while smaller spacing distances lead to a uniform color effect due to a greater angular dispersion.

We have demonstrated the coloration capability of the proposed method and the color pallet generation only on brass workpieces. In fact, the elliptical vibration texturing process due to its intermittent cutting nature can be applied to materials with different machinability, as illustrated in Fig. 7. Surfaces with iridescent effects have been achieved on different materials, such as aluminum alloy, stainless steel and copper. However, the influences of material

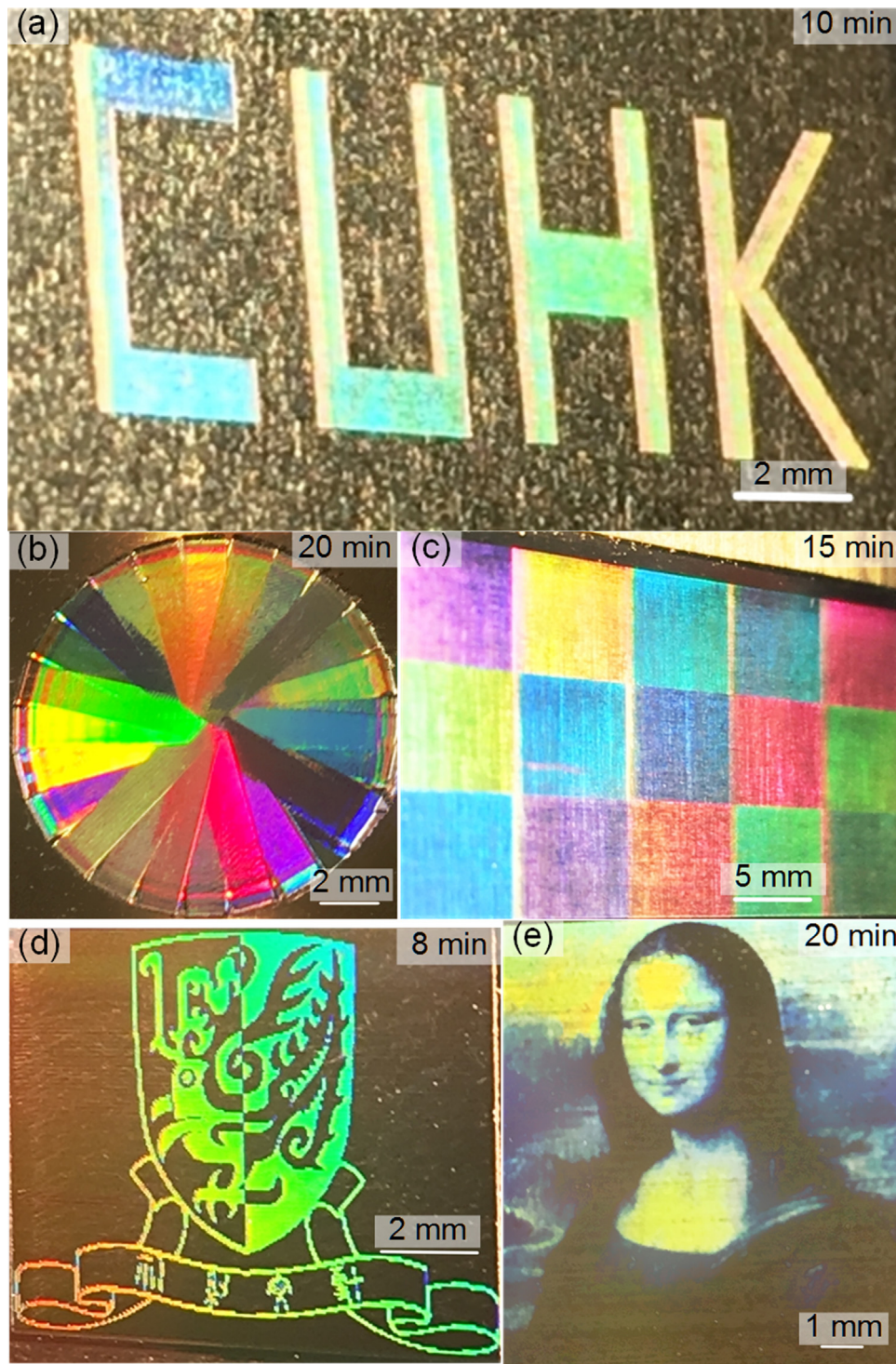


Fig. 10. Pattern and image marking on brass surfaces: (a) patterns by selective texturing; (b) color variation by changing the grating orientation; (c) color blocks by a step velocity profile; (d) the university emblem; (e) the Mona Lisa portrait.

properties on the iridescent effect and tool wear are yet to be determined and are out of the scope of this work.

4.2. Study of the influences of process parameters on the iridescent effect

We performed additional experiments to investigate the spacing distance range capable of achieving iridescent effects and the influence of grating morphologies on the iridescent effect. As ana-

lyzed in the principle section, spacing distance of the periodic micro/nano-ripples is determined by the ratio of nominal cutting velocity to the tool vibration frequency. The vibration frequency is fixed with the resonant frequency of the designed tool and therefore kept as a constant for all texturing experiments. The spacing distance of vibration-induced ripples then can be tuned by choosing a suitable nominal cutting velocity.

As shown in Fig. 8, nominal cutting velocities from the first to the fifth segment were 8.4 mm/s, 16.8 mm/s, 21.0 mm/s, 28.0 mm/s

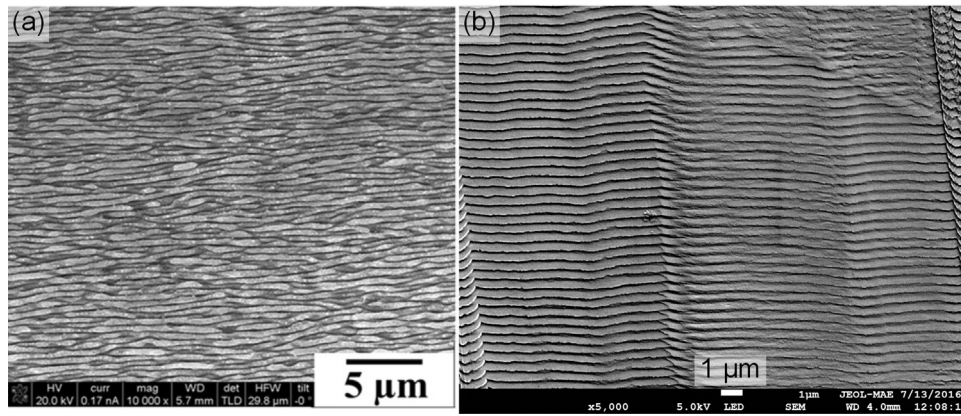


Fig. 11. Comparison between (a) LIPSSs [11] and (b) periodic structures generated by EVT.

Table 1

Process parameters for the study of grating spacing.

Segment no.	Cutting velocity	Spacing distance	
1:	8.4 mm/s	300 nm	
2:	16.8 mm/s	600 nm	
3:	21.0 mm/s	750 nm	
4:	28.0 mm/s	1000 nm	
5:	36.4 mm/s	1300 nm	
Cross feed:	50 μm	Nominal depth-of-cut:	0 μm

and 36.4 mm/s, respectively. The cross feed and depth-of-cut were kept the same for all cases, which were 50 μm and 0 μm. The experimental conditions and results are summarized in Table 1. Different cutting velocities significantly affected the formation of periodic micro/nano-ripples leading to various iridescent effects. The spacing distances of the vibration-induced ripples among the five segments located in the UV light, visible, and near-infrared regions of the spectrum. When viewed at 70°, different segments appeared various colors due to the different grating spacing. In order to study the influence of grating spacing on the iridescent effect and to validate the principle of EVT, surface morphology of all the segments has been examined using a scanning electronic microscope (SEM). As can be seen from Fig. 8(a)–(e), highly regular periodic ripples along the cutting direction were clearly identified on the micrographs. In addition, the ripples were connected in the cross-feed direction forming incessant long edges due to the overlapping of consecutive cuts.

The measured average ripple lengths in each segment were 315 nm, 610 nm, 760 nm, 1050 nm and 1300 nm, corresponding to the theoretical values of 300 nm, 600 nm, 750 nm, 1000 nm and 1300 nm respectively based on Eq. (3). It can be concluded that the texturing results generally capture the theoretical grating spacing. The minute deviation can be attributed to the choice of measurement points, since the periodic length of ripples was varying along the edge.

The ripple edges were connected after sequential cutting parallel lines. The cross feeds should be carefully chosen to form incessant long ripples in the cross feed direction. The width of

micro/nano-ripples in each cutting line was determined by the tool geometry and overall depth-of-cut. If the cross feed was selected smaller than the width of micro/nano-ripples, the projection of the tool geometry in the cutting direction from the two consecutive cuts would be overlapping, thus connecting the ripples in the cross-feed direction. If the cross feed was set larger than the width of micro/nano-ripples, discontinuous ripples would be formed, leading to a deteriorated iridescent effect. In the present study, for a cutting insert of 509 μm nose radius, and 0 depth-of-cut, we chose the cross feed at 50 μm to keep the balance between efficiency and efficacy.

Nominal depth-of-cut was another factor which might influence the iridescent effect. Due to the mechanism of EVT process, the micro/nano-ripples are concurrently generated on machined surfaces. Therefore, within the range of the vibration amplitude, the nominal depth-of-cut has no impact on the final surface textures, thus no effect on the iridescent effect. This conclusion has been verified by our experimental results presented in Fig. 9, where segments with different nominal depth-of-cuts (−3 μm, 0 μm, and 3 μm) exhibit almost the same color viewed at different observation angles. Here we can introduce a negative nominal depth-of-cut to significantly reduce the amount of removed material, which contributes to lower cutting force and reduced effective uncut chip thickness.

4.3. Pattern and image marking

The proposed EVT process also provides the flexibility for color marking on metallic surfaces with arbitrary patterns and images. The spacing distance and grating orientation are the key factors influencing the apparent colors, which are governed by the diffraction grating equation. The samples of pattern and image marking using EVT are demonstrated in Fig. 10. The processing time for each sample is indicated in the figure. Firstly, by controlling the nominal depth-of-cut during the texturing process, we can selectively colorize specific regions of the target surface. Only the regions machined by the vibration cutting tool would exhibit vivid colors, while the remaining regions kept the material's original color, as shown in Fig. 10(a). Secondly, the orientation of the vibration-induced grating can be utilized to control the apparent color. Since the orientation of the gratings determined the incident and diffract angle on the grating equation, various micro-gratings with different grating orientations will exhibit diverse colors even with identical spacing distance, as illustrated in Fig. 10(b).

The nominal cutting velocity can be used to directly control the grating spacing and thus to affect the apparent color. A step velocity profile was used to create color blocks shown in Fig. 10(c). Since the nominal cutting velocity profile can be easily programmed in G-code, high-resolution and complex patterns can be generated accordingly. As an example, the emblem of the Chinese University of Hong Kong (CUHK) was textured using two different grating spacing values (Fig. 10(d)). The designed resolution, or single pixel size, was $40 \times 40 \mu\text{m}$, which could not be discernible by human eyes at a normal viewing distance. Another multicolor image of the Mona Lisa portrait was reproduced in Fig. 10(e) with a $40 \times 40 \mu\text{m}$ pixel size. The RGB values of the original image were taken and categorized into 16 different levels. The 16 levels were evenly distributed between 500 nm to 1000 nm in terms of the grating spacing distance, which meant that 0 RGB value was corresponding to 500 nm; while the 255 was assigned to 1000 nm.

The resolution capability of the proposed process is anisotropic, so that it has a very high resolution in the cutting direction (submicron level), which is only constrained by the acceleration capability and accuracy of the motion stage. The cross feed resolution (line width) is a function of the cutting tool geometry, which could reach 2–3 μm for a commercially available flat tip diamond cutting insert. The relationship between the process efficiency and resolution is also very unique. The processing time is irrelevant to the resolution in the cutting direction, but only linearly increases with the resolution in the cross feed direction (or the cutting width). Furthermore the processing time is only slightly affected by the number of color choices.

5. Conclusion

The proposed method, elliptical vibration texturing for structural coloration, is highly flexible. It is in essence a micro-machining process, which has been well developed to process free-form surfaces [19] and multi-materials (glass, metals, ceramics, etc.) [20]. Due to the interrupted cutting of EVT, it is also favorable for processing difficult-to-machine and brittle materials [21–23].

The proposed method can be directly compared with the femtosecond laser based technique. The major advantage of the proposed method over the laser process is a better iridescent effect due to a much more regular periodic structures and a higher diffraction efficiency. Typical SEM images of laser-induced LIPSSs [11] and periodic structures machined by the proposed method are compared in Fig. 11. It could be seen that the periodic ripples induced by EVT are statistically more controlled and regular, thus enhancing the iridescent effect. The grating spacing could be analytically

predicted irrelevant to the workpiece material since the proposed method is based on mechanical machining; while for the laser process, a calibration procedure is always required for each different combination of process parameters, laser source, and workpiece materials. Moreover, due to the overlapping of elliptical vibration tool trajectories, micro/nano-structures are induced concurrently during the removal of a thin layer of workpiece material. As a consequence, no extra pre-machining, polishing, or post-processing procedures are required. Compared to the sample preparation for the laser process, workpieces with relative large surface roughness are acceptable for direct coloration process using the EVT technique.

In summary, an innovative mechanical machining method, termed elliptical vibration texturing, is proposed for fast and precise structural coloration on metallic surfaces in this paper. Preliminary iridescent effects of texts and patterns have been achieved on metallic surfaces using the proposed method. The principle of elliptical vibration texturing and the mechanism of micro/nano-structure generation are explained. The textured results are systematically analyzed and verified. Influences of different process parameters, namely cutting velocity, cross feed and nominal depth-of-cut, on the generated micro-gratings have been studied and discussed. The grating resolution and iridescent effect are associated with the spacing distance, which can be readily controlled by adjusting the nominal cutting velocity during the coloration process to reproduce complex image and patterns.

Acknowledgements

This work has been supported by the Innovation and Technology Fund, Hong Kong, #ITS/014/15; a grant from The Chinese University of Hong Kong, #3132823; and Research Grants Council of Hong Kong, #ECS 24201816.

References

- [1] A. Bruzzone, H. Costa, P. Lonardo, D. Lucca, Advances in engineered surfaces for functional performance, *CIRP Ann. Manuf. Technol.* 57 (2008) 750–769.
- [2] B. Dussler, Z. Sagan, H. Soder, N. Faure, J.-P. Colombier, M. Jourlin, E. Audouard, Controlled nanostructures formation by ultra fast laser pulses for color marking, *Opt. Express* 18 (2010) 2913–2924.
- [3] J. Liu, J.P. Coleman, Nanostructured metal oxides for printed electrochromic displays, *Mater. Sci. Eng.: A* 286 (2000) 144–148.
- [4] T. Ergin, N. Stenger, P. Brenner, J.B. Pendry, M. Wegener, Three-dimensional invisibility cloak at optical wavelengths, *Science* 328 (2010) 337–339.
- [5] S. Kinoshita, S. Yoshioka, J. Miyazaki, Physics of structural colors, *Rep. Prog. Phys.* 71 (2008) 076401.
- [6] T. Xu, Y.-K. Wu, X. Luo, L.J. Guo, Plasmonic nanoresonators for high-resolution colour filtering and spectral imaging, *Nat. Commun.* 1 (2010) 59.
- [7] S.J. Tan, L. Zhang, D. Zhu, X.M. Goh, Y.M. Wang, K. Kumar, C.-W. Qiu, J.K. Yang, Plasmonic color palettes for photorealistic printing with aluminum nanostructures, *Nano Lett.* 14 (2014) 4023–4029.
- [8] T. Kita, T. Harada, Ruling engine using a piezoelectric device for large and high-groove density gratings, *Appl. Opt.* 31 (1992) 1399–1406.
- [9] E. Palmer, M. Hutley, A. Franks, J. Verrill, B. Gale, Diffraction gratings (manufacture), *Rep. Prog. Phys.* 38 (1975) 975.
- [10] A.Y. Vorobyev, C. Guo, Colorizing metals with femtosecond laser pulses, *Appl. Phys. Lett.* 92 (2008) 041914.
- [11] M.S. Ahsan, F. Ahmed, Y.G. Kim, M.S. Lee, M.B. Jun, Colorizing stainless steel surface by femtosecond laser induced micro/nano-structures, *Appl. Surf. Sci.* 257 (2011) 7771–7777.
- [12] J. Long, P. Fan, M. Zhong, H. Zhang, Y. Xie, C. Lin, Superhydrophobic and colorful copper surfaces fabricated by picosecond laser induced periodic nanostructures, *Appl. Surf. Sci.* 311 (2014) 461–467.
- [13] Z. Ou, M. Huang, F. Zhao, Colorizing pure copper surface by ultrafast laser-induced near-subwavelength ripples, *Opt. Express* 22 (2014) 17254–17265.
- [14] X. Liu, R.E. DeVor, S. Kapoor, K. Ehmann, The mechanics of machining at the microscale: assessment of the current state of the science, *J. Manuf. Sci. Eng.* 126 (2004) 666–678.
- [15] X. Liu, R. DeVor, S. Kapoor, An analytical model for the prediction of minimum chip thickness in micromachining, *J. Manuf. Sci. Eng.* 128 (2006) 474–481.
- [16] P. Guo, K.F. Ehmann, An analysis of the surface generation mechanics of the elliptical vibration texturing process, *Int. J. Mach. Tools Manuf.* 64 (2013) 85–95.

- [17] P. Guo, Y. Lu, P. Pei, K.F. Ehmann, Fast generation of micro-channels on cylindrical surfaces by elliptical vibration texturing, *J. Manuf. Sci. Eng.* 136 (2014) 041008.
- [18] P. Guo, K.F. Ehmann, Development of a tertiary motion generator for elliptical vibration texturing, *Precis. Eng.* 37 (2013) 364–371.
- [19] X. Luo, K. Cheng, D. Webb, F. Wardle, Design of ultraprecision machine tools with applications to manufacture of miniature and micro components, *J. Mater. Process. Technol.* 167 (2005) 515–528.
- [20] D. Dornfeld, S. Min, Y. Takeuchi, Recent advances in mechanical micromachining, *CIRP Ann. Manuf. Technol.* 55 (2006) 745–768.
- [21] X. Zhang, A.S. Kumar, M. Rahman, C. Nath, K. Liu, Experimental study on ultrasonic elliptical vibration cutting of hardened steel using PCD tools, *J. Mater. Process. Technol.* 211 (2011) 1701–1709.
- [22] N. Suzuki, M. Haritani, J.-b. Yang, R. Hino, E. Shamoto, Elliptical vibration cutting of tungsten alloy molds for optical glass parts, *CIRP Ann. Manuf. Technol.* 56 (2007) 127–130.
- [23] C. Nath, M. Rahman, K. Neo, A study on ultrasonic elliptical vibration cutting of tungsten carbide, *J. Mater. Process. Technol.* 209 (2009) 4459–4464.